CAAP Quarterly Report

Date of Report: 01/11/2019

Prepared for: *U.S. DOT Pipeline and Hazardous Materials Safety Administration*

Contract Number: 693JK31850008CAAP

Project Title: Fluorescent Chemical Sensor Array for Detecting and Locating Pipeline Internal Corrosive Environment

Prepared by: Dr. Ying Huang and Dr. Wenfang Sun

Contact Information: Dr. Ying Huang, Email: ying.huang@ndsu.edu, Phone: 701.231.7651

For quarterly period ending: Jan. 07, 2019

Business and Activity Section

(a) Contract Activity

Discussion about contract modifications or proposed modifications

None.

Discussion about materials purchased

None.

(b) Status Update of Past Quarter Activities

In this quarter, the university research team completed Task 1 of the above mentioned project, including a kick-off meeting with PHMSA program managers on Nov. 15th, 2018 and a thorough literature review on related topics to respond to the PHMSA program managers' comments from the kick-off meeting, in addition to hiring three graduate students and two undergraduate students for the project and an outreach event to middle school students as "Pipeline Challenge" in BrainSTEM on Oct. 24th, 2018 to expand the educational impact of this project.

(c) Cost share activity

None.

(d) Task 1: Literature Review & Kick-off Meeting

In this task, four activities were performed, including (1) a kick-off meeting with PHMSA personnel held on Nov. 15th, 2018 to ensure that the project objectives and tasks follow the DOT and PHMSA's expectations and guidelines; (2) a thorough literature review performed on related topics of the proposed research, which included but not limited to the pipeline internal corrosion detection techniques, existing fluorescent chemical sensors for different chemicals related to internal corrosion, their limitations and advantages, and current internal corrosion detection using smart pigs or inline inspection (ILI) tools; (3)

hiring three graduate students and two undergraduate researchers to work on this project; and (4) an outreach event conducted to middle school students on Oct. 24th, 2018 as "Pipeline Challenge" outreach project.

1. Background and Objectives in the 1st Quarter

1.1 Background

This project is designed to develop passive colorimetric/fluorescent chemical sensor array for locating and detecting corrosive water inside pipes. Inside the pipelines, the transported crude oil may include a hot mixture of free water, carbon dioxide (CO_2), hydrogen sulfide (H_2S) and microorganisms. The different chemical components inside oil/water environment such as HCO_3^- / CO_3^{2-}, Fe^{3+}, S^{2-}, H^+ or pH may result in different internal corrosion mechanisms, such as sweet corrosion or sour corrosion. The passive colorimetric/fluorescent sensor array to be developed in this project is intended to detect the concentration changes of the five above mentioned important chemical species in the internal oil/water environment of the pipeline and use these detected environmental data to predict the internal corrosion progressing of pipelines. In the first quarter of this project, literature review was expected to direct the research to the right direction for sensor array development in future quarters.

1.2 Objectives in the 1st Quarter

In the first quarter, the major objective is to effectively communicate with PHMSA personnel to understand the specific requirements. More specifically, there are two sub-objectives as aligned in the proposal:

(1) Kick-off meeting with PHMSA personnel to ensure that the project objectives and tasks follow the DOT and PHMSA's expectations and guidelines;

(2) Literature review on related topics of the proposed research, including but not limited to the pipeline internal corrosion detection techniques, existing fluorescent chemical sensors for different chemicals related to internal corrosion, their limitations and advantages, and current internal corrosion detection using smart pigs or ILI tools.

2. Results and Discussions

2.1 Kick-off Meeting

On Nov. 15th, 2018 (10:30 am-12:00 pm), a video kick-off meeting was conducted between the PHMSA program managers and the research team. All three PIs, Dr. Huang, Dr. Sun, and Dr. Wang, attended the kick-off meeting. A web presentation was made to the PHMSA personnel followed by questions / answers and discussions. Five questions were discussed during the kick-off meeting as following:

1. How to quantify the corrosive species detected by the sensor? (Question #1)
2. Which corrosion model will be used to run the sensor monitoring results? (Question #2)
3. How to install sensors onto pipe interior surface, need cut off the line or just drill hole? (Question #3)
4. What's the sensor size? If the sensor could be destroyed/damaged by the cleaning pig, or stuck the ILI tool if the sensor reduce the pipe ID. (Question #4)
5. If an operator for field test has been identified? If a shutting down of the pipeline will be needed for sensor installation? (Question #5)

2.2 Literature Review

Responding to the comments and questions (Question #1 ~ #5) from PHMSA personnel in the kick-off meeting, a thorough literature review was performed on four topics on colorimetric/fluorescent

chemical sensors, internal corrosion prediction model analysis, intrusive internal corrosion detection and its sensor installation methods, inline inspection tools, and pipeline utility pigs. The detailed reviews on these topics are provided below. As the project moves forward, more specific answers to the comments/questions will be further addressed.

2.2.1 Colorimetric/fluorescent chemical sensor (Question #1)

The chemical sensor array to be developed in this project will detect the concentrations of CO_3^{2-} / HCO_3-, S^{2-}, Fe^{3+}, and H^+/OH^- quantitatively using color changes which are expected to be recorded from cameras from the ILI tools (reviewed in Section 2.2.4). To develop such chemical sensor array, literature review was performed on detecting each chemical species including CO_3^{2-} / HCO_3-, S^{2-}, Fe^{3+}, and H^+/OH^- as provide in the following subsections.

2.2.1.1 Fluorescent Chemical Sensor for Detecting CO_3^{2-} / HCO_3-: One of the fluorogenic signaling probe for the carbonate (CO_3^{2-}) / bicarbonate (HCO_3^-) ions was reported by Ki Hwan Lee's group (structure (a) in Figure 1(a)).[1] Upon addition of CO_3^{2-} or HCO_3^- ions, the intensity of the fluorescence emission signal at 424 nm was greatly enhanced, accompanied by a color change from yellow to purple. The proposed mechanism is given in Figure 1(a).

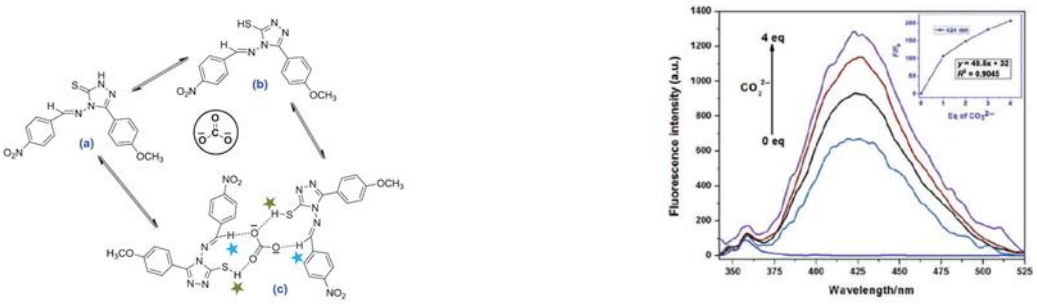

(a) (b)

Figure 1. (a) The structure of carbonate ion sensor and the proposed binding mechanism with carbonate ion. (b) Fluorescence intensity change with the addition of carbonate ions into the probe solution.

Yue-Peng Cai's group developed lanthanide complexes with two analogous diimine ligands.[2] The structures of the complexes are given in Figure 2(a). The DMSO solution of these two complexes exhibited a specific and prompt fluorescence response to CO_3^{2-} with a significant color and intensity change as shown in Figure 2(b).

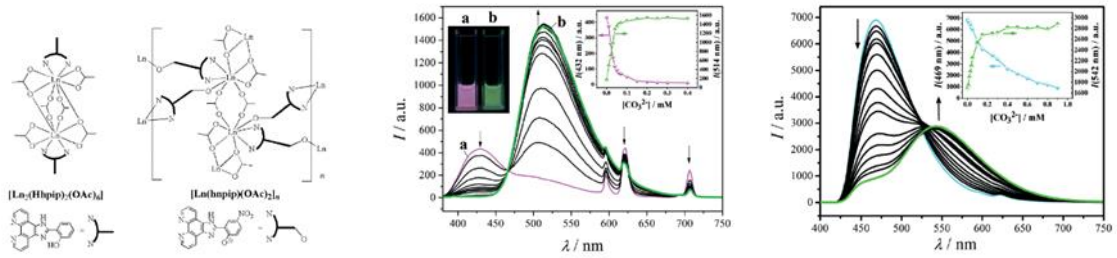

(a) (b) (c)

Figure 2. (a) Structural illustration for the lanthanide complexes. (b) Fluorescence intensity changes with the addition of carbonate ions into a DMSO solution of $[Eu_2(pip)_2OAc)_6]$. (c) Fluorescence intensity changes with the addition of carbonate ions into a DMSO solution of $[Eu_2(Hhpip)_2OAc)_6]$.

Ute Resch-Genger's group reported a series of structurally simple, fluorescent sensor molecules based on the iminoylthiourea/1,2,4-thiadiazole unit, which showed a significant fluorescence intensity enhancement for CO_3^{2-} and HCO_3^- due to the formation of hydrogen bonds between the NH groups of the central guanidyl moiety and the CO_3^{2-} / HCO_3^- anions.[3] Figure 3 shows the structures of the

fluorescent senor molecules (a), proposed sensing mechanism with compound **3** (b), and fluorescence intensity change in the presence of various anions (c).

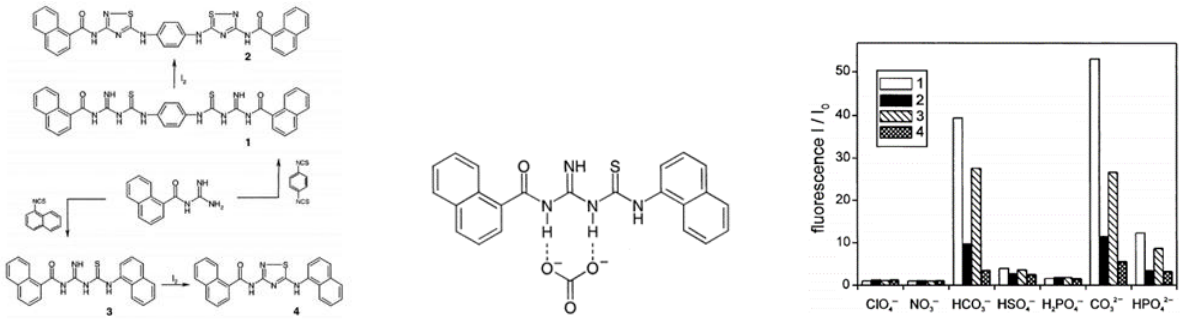

(a) (b) (c)

Figure 3. (a) Synthesis of the anion receptors **1** and **3** (reduced forms), and **2** and **4** (oxidized forms). (b) Proposed model structure for the CO_3^{2-}-**3** complex. (c) Fluorescence intensity change in the presence of various anions.

A new fluorescent nano-sensor for CO_3^{2-} ion detection was developed based on the CdSe quantum dots (QD).[4] The chromophore-modified quantum dots allowed a selective fluorescence "turn-on" response toward CO_3^{2-} ion, and the proposed mechanism is provided in Figure 4(a). The quantum dots show a distinct selectivity toward CO_3^{2-} ion (Figure 4(b)).

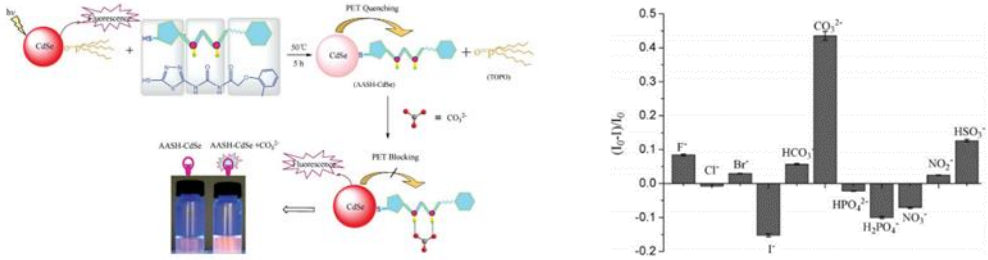

(a) (b)

Figure 4. (a) Synthetic procedure for chromophore-modified CdSe QDs and the proposed mechanism for CO_3^{2-} ion recognition. (b) Ratios of the fluorescence intensity change of CdSe QDs upon addition of relevant anions.

Another fluorescent colorimetric chemo sensor for detection of CO_3^{2-} ions is based on a novel bis-Schiff base compound.[5] The ^{1}H NMR and mass spectrometry studies confirmed that the presence of two terminal hydroxyl groups played an essential role in the sensing mechanism. This sensor molecule showed a significant emission enhancement at 398 nm. As shown in Figure 5(c), it can specifically respond to CO_3^{2-} ions among a variety of other anions.

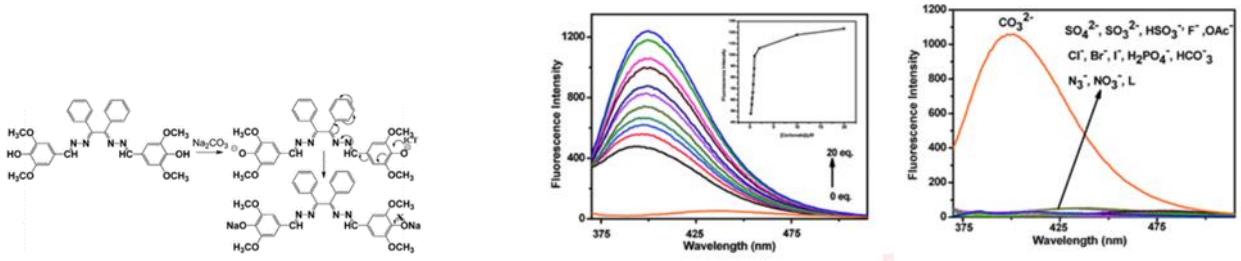

(a) (b) (c)

Figure 5. (a) Structure of the sensor molecule and proposed sensing mechanism. (b) Fluorescence spectra of sensor molecule after addition of CO_3^{2-}. (c) Fluorescence spectra of sensor molecule before and after addition of various anions.

2.2.2.2 Fluorescent Chemical Sensor for Detecting S^{2-}: Suk-Kyu Chang's group reported a new fluorescence "turn-on" sulfide sensor based on a Cu^{2+} complex (Figure 6(a)).[6] Addition of Cu^{2+} into

the sensor solution resulted in highly stable CuS precipitate, which turn-on the fluorescence from the free ligand (Figure 6(b)). This sensor showed a specific response toward S^{2-} (Figure 6(c)).

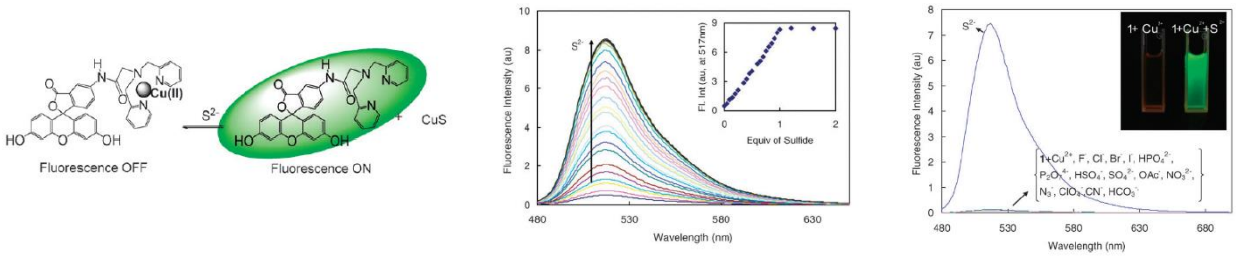

(a) (b) (c)

Figure 6. (a) Chemical structure of the sensor and the sensing mechanism. (b) Titration experiment with S^{2-}. (c) Fluorescence changes of sensor in the presence of various anions.

Based on the similar idea, Zhengzhi Zeng's group reported another Cu^{2+} complex based fluorescent sensor for S^{2-} anion.[7] With the addition of Cu^{2+}, the color of the ligand changed from orange to yellow. Meanwhile, the green emission from the ligand was quenched. After adding S^{2-} anion, the color changed back to orange and the green emission was "switched on".

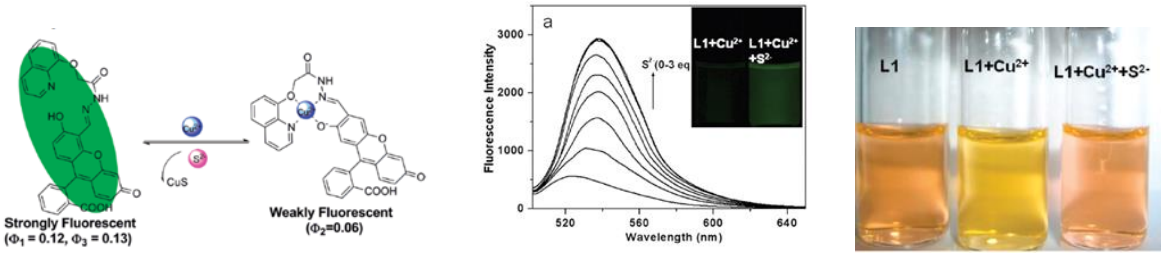

(a) (b) (c)

Figure 7. (a) Proposed sensing mechanism. (b) Changes of fluorescence intensity upon the addition of S^{2-}. (c) Photographs of color change.

Tetsuo Nagano's group developed another Cu^{2+} complex based fluorescence sensor HSip-1 (structure shown in Figure 8(a)) for S^{2-}.[8] This sensor showed high sensitivity toward S^{2-} (Figure 8(c)) with a significant fluorescence intensity increase at 516 nm after adding 100 μM Na_2S (Figure 8(b)).

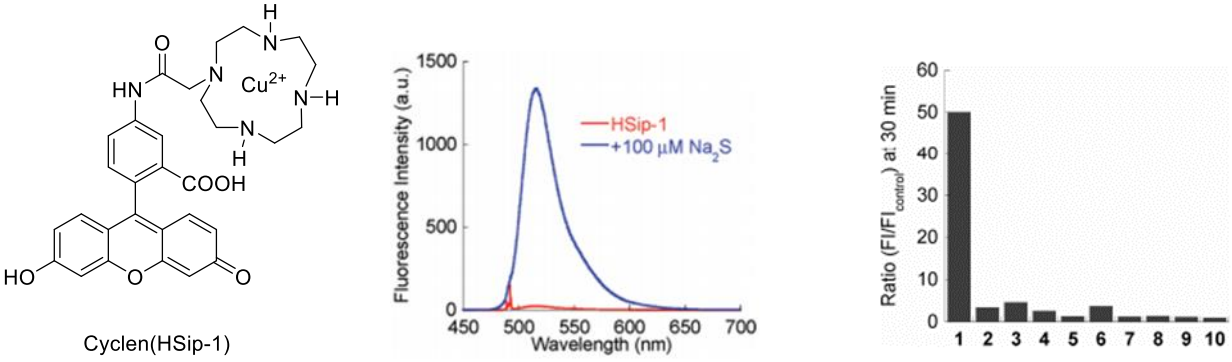

(a) (b) (c)

Figure 8. (a) Structure of HSip-1. (b) Fluorescence spectra of Hsip-1 before (red) and after (blue) addition of Na_2S. (c) Fluorescence enhancement of the sensor in the presence of thiols, inorganic sulfur compounds, and sodium ascorbate. (1) Na_2S, (2) GSH, (3) L-Cys, (4) DL-Hcy, (5) 2-ME, (6) DTT, (7) NaSCN, (8) Na_2SO_3, (9) $Na_2S_2O_3$, and (10) sodium ascorbate

Yong Qian's group reported two sulfide-selective fluorescent probes, SFP-1 and SFP-2, for live-cell sulfide detection.[9] A significant fluorescence increase was observed after adding H_2S or Na_2S in SFP-1 and SFP-2 (Figure 9(b) and (d)). They both exhibited effective detection for sulfide generation from enzymes and excellent cell-based sulfide imaging in live cells in the presence of thiols.

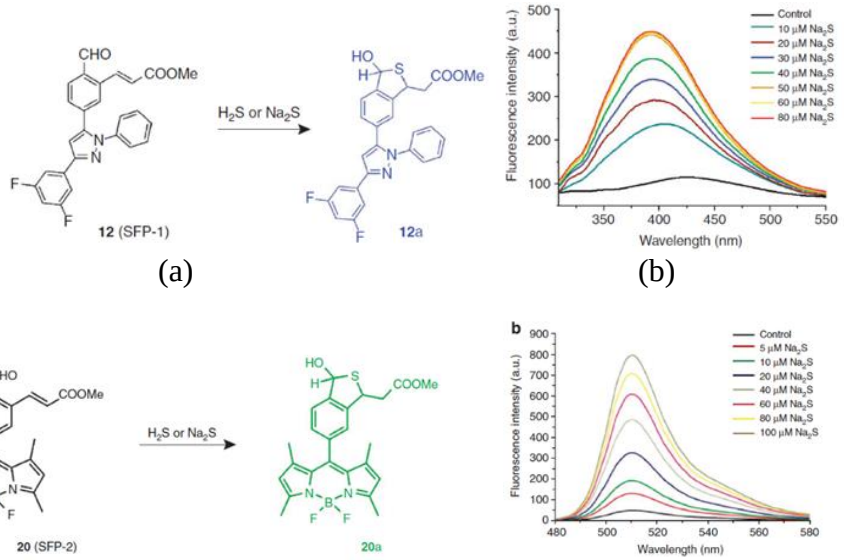

Figure 9. (a) Structure and sensing mechanism of SFP-1. (b) Fluorescent intensity change of SFP-1 upon addition of Na_2S. (c) Structure and sensing mechanism of SFP-2. (d) Fluorescent intensity change of SFP-2 upon addition of Na_2S.

Christopher J. Chang's group reported a pair of new reaction-based fluorescent sensors (SF1 and SF2) for H_2S generated from living cells.[10] Both sensors exhibited a high selectivity toward H_2S in both water and living cells. As shown in Figure 10, the fluorescence intensity significantly increased at 488 nm for SF1 and SF2 with addition of H_2S.

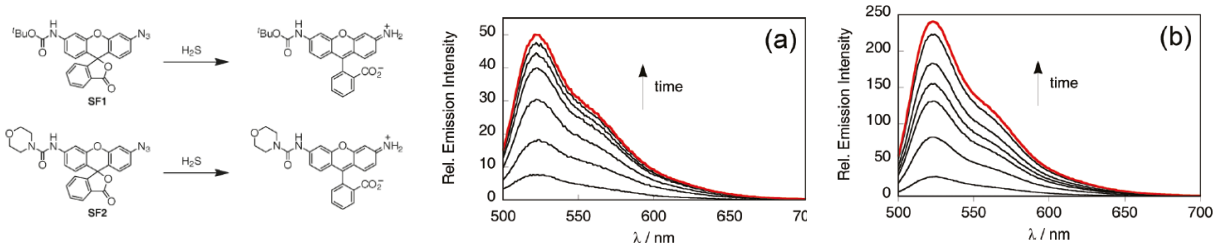

Figure 10. (a) Chemical structure of SF1 and SF2. (b) Fluorescence response of SF1 to H_2S. (c) Fluorescence responses of SF2 to H_2S.

2.2.2.3 Fluorescent Chemical Sensor for Detecting Fe^{3+}: To detect Fe^{3+}, a highly selective and ultrasensitive fluorescence "turn-on" sensor 4-pyridin-2-ylmethyleneaminophenol (PYAP) was developed by Sen's group.[11] In the presence of 2 equiv. of Fe^{3+}, a 200-fold increase of fluorescence intensity was observed for PYAP (Figure 11(b)); while the other metal ions, such as Na^+, K^+, Ba^{2+}, Mg^{2+}, Al^{3+}, Cr^{3+}, Co^{2+}, Ni^{2+}, Cu^{2+}, Zn^{2+}, Cd^{2+}, Pb^{2+} and Ag^+ only induced a minor change in the fluorescence intensity.

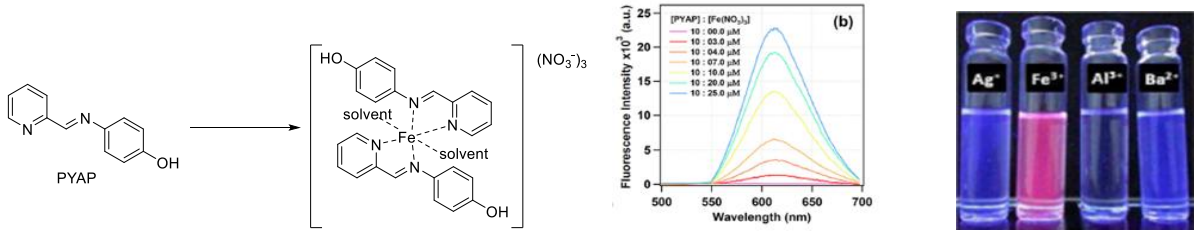

Figure 11. (a) Chemical structure of PYAP. (b) Fluorescence spectra of PYAP upon addition of Fe^{3+}. (c) Fluorescence turn-on for Fe^{3+} detection.

John H. Xin's group reported a bis-rhodamine derivative BRU sensor (Figure 12(a) for Fe^{3+} ions.[12]

The fluorescence intensity was significantly enhanced in the presence of Fe^{3+} (Figure 12(b)). BRU showed a high recognition toward Fe^{3+}. In addition, after addition of the carbonate anion, the generated BRU-Fe^{3+} complex displayed a fluorescence quench (Figure 12(c)).

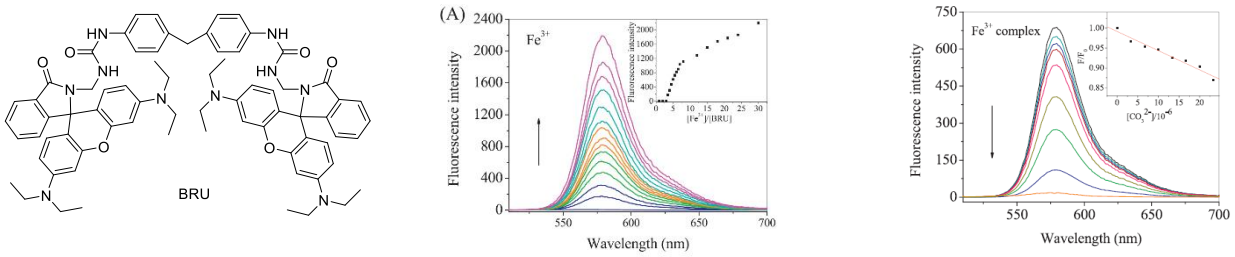

(a) (b) (c)

Figure 12. (a) Chemical structure of BRU. (b) Fluorescence spectra of BRU upon addition of Fe^{3+}. (c) Fluorescence titration of BRU-Fe^{3+} solution with carbonate.

Aijun Tong's group reported another rhodamine 6G based Fe^{3+} ion sensor (Figure 13(a)).[13] This Fe^{3+} sensor showed a high selectivity toward Fe^{3+} over other metal ions (Figure 13(b)). After adding Fe^{3+}, the spirocyclic ring of the sensor molecule opened and coordinated with the Fe^{3+} ions, exhibiting a significant enhancement of the fluorescence intensity at 560 nm in water and ethanol (Figure 13(a)).

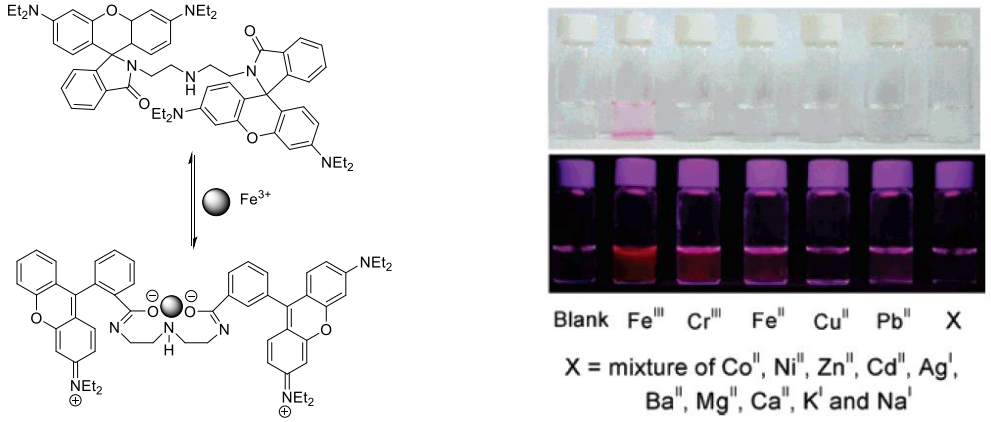

(a) (b)

Figure 13. (a) Chemical structure of the sensor and the proposed sensing mechanism. (b) Color change and fluorescence "turn-on" for Fe^{3+} detection.

Shouheng Sun's group also developed a rhodamine 6G based PEG-Fe_3O_4 nanoparticle **1b** and used it for Fe^{3+} detection in water (Figure 14(a)).[14] After adding Fe^{3+} ion into **1b**, the spirocyclic ring was converted into the open-ring form and coordinated with Fe^{3+}, giving rise to a significant fluorescence enhancement at 550 nm. This sensor showed a good sensitivity and selectivity toward Fe^{3+}.

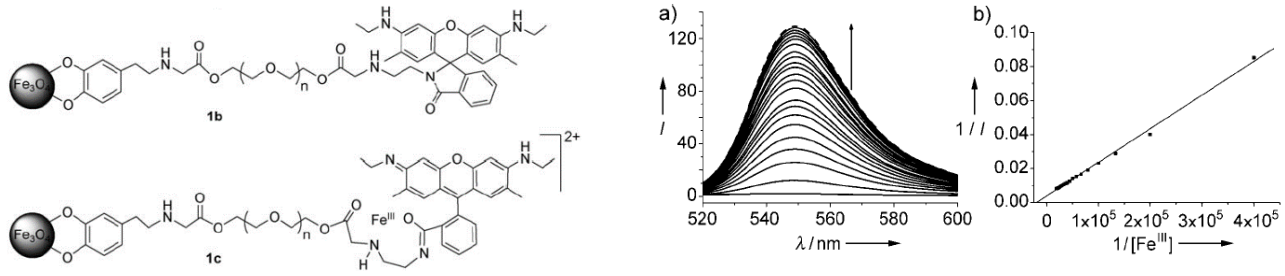

(a) (b)

Figure 14. (a) Chemical structure of **1b**. (b) Fluorescence enhancement of **1b** upon addition of Fe^{3+}.

2.2.2.4 Fluorescent Chemical Sensor for Detecting H^+/OH^-: A square-planar Pt(II) complex **2** (Figure

15(a)) was reported by Sun's group.[15] This complex exhibited a purple color and essentially non-emissive in its original form. However, in acidic solutions, the dimethylamino($N(CH_3)_2$) group was protonated and the nature of the lowest singlet and triplet excited states changed, resulting in a dramatic color change from purple to yellow and the emission was turned on at 510 nm as shown in Figure 15(b) and (c). In contrast, the color of complex **2** changed to blue under basic conditions, and the emission was completely quenched.

(a) (b) (c)

Figure 15. (a) Chemical structure of complex **2**. (b) Color change of **2** under acidic and basic conditions. (c) Emission "turn-on" for H^+ detection.

A Ru (II) complex $[(bpy)_2Ru(aip)](ClO_4)_2\ H_2O$ (Figure 16(a)) reported by Ke-Zhi Wang's group [16] also exhibited pH-dependent emission changes (Figure 16(b) and (c)). Increasing the pH from 0.05 to 4.00 caused a blue-shift of the emission band from 633 nm to 609 nm accompanied by an increased intensity. Upon further increasing the pH from 6.00 to 10.5, the emission band red-shifted from 613 nm to 617 nm and the emission intensity decreased. However, neither the emission color nor the intensity change was significant.

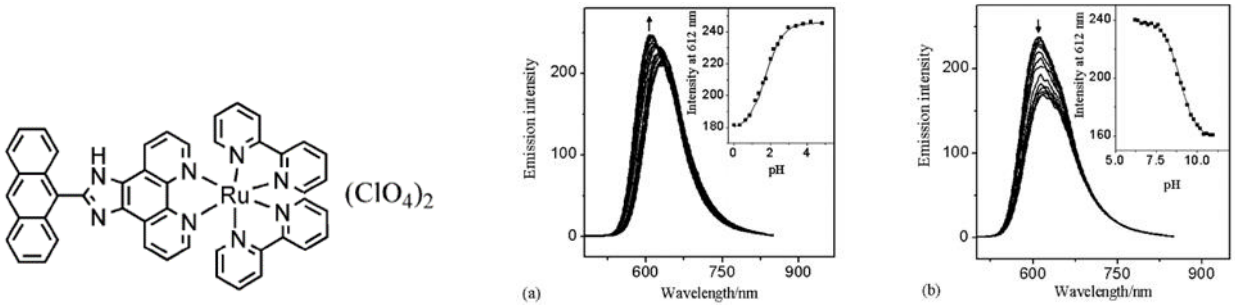

(a) (b) (c)

Figure 16. (a) Chemical structure of the Ru(II) complex. (b) The impact of pH value on the emission spectra of the Ru(II) complex in the range of 0.05-4.00. (c) The impact of pH value on the emission spectra of the Ru(II) complex in the range of 6.00-10.5.

Li-Hua Gao's group [17] reported another Ru(II) complex, $[Ru(bpy)_2(dhipH_3)](ClO_4)_2$, which showed a significant pH response. The process of protonation and deprotonation of this complex (Figure 17(a)) influenced the emission properties of the complex (Figure 17(b)), which can be used as a pH indicator.

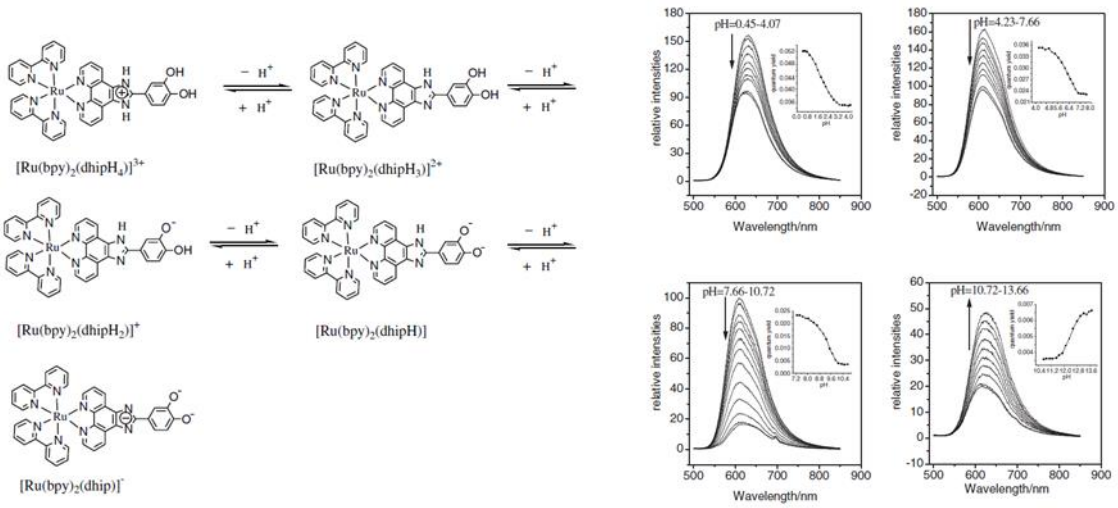

(a) (b)

Figure 17. (a) Molecular structure and protonation/deprotonation process of Ru(II) complex. (b) The pH effect on emission spectra of the Ru(II) complex.

Recently, an 8-hydroxyquinoline-functionalized covalent organic framework (COF-HQ) was reported by Wang's group [18] (Figure 18(a)). The fluorescent intensity of COF-HQ decreased as the pH decreased (Figure 18(b)). Protonation of COF-HQ broke the π-conjugation system of HQ (Figure 18(c)) and led to emission quenching. The sensor solution color changed from bluish-purple to yellow as the pH increased (Figure 18(d)).

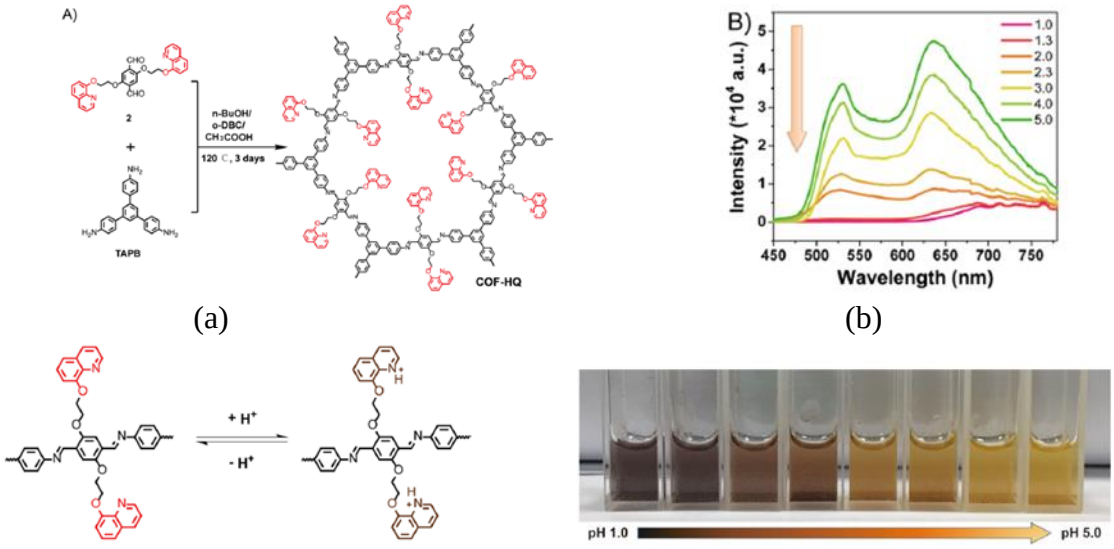

(a) (b)

(c) (d)

Figure 18. (a) Chemical structure of COF-HQ. (b) The pH effect on emission intensity of COF-HQ. (c) Sensing mechanism. (d) Color changes of COF-HQ at different pH values.

Based on the review, it can be seen that it is very positive that chemical sensors based on color or emission color/intensity changes can be developed to detect corrosion related chemical species including CO_3^{2-} / HCO_3-, S^{2-}, Fe^{3+}, and H^+/OH^- as proposed in this project.

2.2.2 Internal corrosion prediction model analysis (Question #2)

To design a pipeline, it is required to calculate the minimum wall thickness following appropriate standards,[19-20] which includes wall thickness needed for pressure containment and corrosion allowance.[21] Corrosion allowance considers the pipe wall thickness loss due to corrosion which can be set either using predicted corrosion rate and design life of the pipeline or experience. Pipeline internal

corrosion prediction models use all the corrosion influencing factors available inside a pipe to predict the corrosion rate. Although a true industry standard approach to exactly predict the pipeline internal corrosion does not exist, there are numerous models developed trying to perform quantitative prediction on the corrosion rate.[22,23] These corrosion rate models can be categorized into mechanistic, semi-empirical, and empirical models.[24]

Mechanistic models describe the mechanisms of the underlying reactions and have a strong theoretical background. Most of the constants appearing in this type of models have a clear physical meaning. Many of the constants are easily found in the literature, while some have still to be obtained by comparing the predictions with available experiments.[24] De Waard and Milliams firstly proposed the mechanistic corrosion rate equation as a function of the temperature and the partial pressure of CO_2 for sweet corrosion in 1975 (noted as De Waard model).[25] The model includes an on/off factor for oil wetting in crude oil systems, which is turned off when the water cut is below 30% and the liquid velocity is above 1 m/s. There are other mechanistic corrosion prediction models based on thermodynamic with electrochemical model, such as OLI Model (or Anderko model),[26,27] which does not consider any effect of oil wetting.

Semi-empirical models are only partly based on firm theoretical hypotheses. They are for practical purposes extended to areas where insufficient theoretical knowledge is available in a way that the additional phenomena are described with empirical functions. Some of the constants appearing in these models have a clear physical meaning while others are arbitrary best-fit parameters.[24] For example, the De Waard model was further modified into a semi-empirical model to account for other environmental factors such as protective layers, pH value, and flow velocity in 1991 and 1995.[28-30] More correction factors have been added into the De Waard model after that to improve the accuracy of the prediction such as the ECE model[31,32] developed by Intetech to include pH from the water chemistry and effects of small amounts of H_2S and acetic acid for well and flowline, the KSC model developed at Institute for Energy Technology[33-35] based on electrochemical model without consideration of oil wetting, the Predict model[36-38] developed by InterCorr International to include strong effects of oil wetting and variation in pH, and the Cassandra model[39,40] developed by BP to include pH calculation. The KSC model was developed further as Multicorp model[41-43] by including modeling of multiphase flow, precipitation of iron carbonate films and effects of oil wetting and crude oil chemistry and H_2S, and verified against laboratory and field data, which is also available as commercial software to be used.

In addition to mechanistic and semi-empirical models, there are some empirical corrosion rate prediction models. The empirical models have very little or no theoretical background. Most constants used in them have no physical meanings – they are just best-fit parameters to the available experimental results. When calibrated with a very large and reliable experimental database, these models can give good interpolation.[24]. There are many empirical models such as the Norsok M-506 Model[44-48], the Hydrocor[49-52] and SweetCor[53] models developed by Shell, the Corplus[53-56] model, and the probabilistic model.[57,58] These empirical models considered the effects from the concentration of O_2, partial pressure of CO_2 and H_2S, and pH for CO_2/H_2S corrosion. The Norsok M-506 model[44] was formed to be a corrosion rate standard in Norwegian petroleum industry, which has a very wide application in the oil/gas corrosion rate prediction. The basic corrosion rate between 20 °C to 150 °C from the Norsok M-506 model can be predicted as:[44,45]

$$C_{rt} = K_t^* f_i^* \left(\frac{S}{19}\right)^{0.146+0.0324\log f_i} * f(pH)t \ \text{(mm/yr)}. \qquad (1)$$

where, C_{rt} is the corrosion rate at temperature t in mm/year, k_t is the constant for the temperature t used in corrosion rate calculations, f is the friction factor, S is the wall shear stress in Pa, and f(pH)t is the pH factor at temperature t.

The probabilistic model is a data-driven empirical model which requires significantly large amount of data for prediction. These probabilistic models can predict both uniform and pitted corrosion rate, which include random variable-based models, such as linear and non-linear random variable-based

models, and stochastic process-based models, such as linear stochastic process, non-linear stochastic process, Markov process and Gamma process.[58] The linear random variable-based model which is the simplest probabilistic approach and also is the most commonly used approach in the industry that usually overestimates the pitted corrosion growth rate while the non-linear random variable-based model considers the non-linear behavior of corrosion process.[59] None of these random variable-based models consider spatial heterogeneity, temporal variation, and measurement errors. The two stochastic process-based models on the other hand do not consider spatial heterogeneity and measurement errors.[60] The Markov process-based models consider epistemic uncertainty, temporal variability, non-linearity and also depth dependency of the corrosion rates.[61] However, the spatial heterogeneity and measurement uncertainties are not addressed properly. The gamma process-based models are the most versatile models that can address different levels of uncertainties.[62] Besides, they can model the non-linearity in the corrosion growth process. These models can also be updated properly by Bayesian inference in case of new imperfect ILI data. Also, to improve the accuracy of the probabilistic empirical corrosion prediction models, optimization algorithms, such as back propagation (BP), genetic algorithm (GA), particle swarm optimization, and artificial neural networks (ANN), can also be used.[63-66] Application of these optimization algorithms enables nondeterministic analysis on the available data for corrosion rate prediction. Among all the optimization algorithms, ANN is the most popularly used algorithm due to the fact that ANN is a non-linear data modeling tool, and it is usually utilized to model complex statistical relationships between inputs and outputs.[67-69]

Among three classes of corrosion rate models, most corrosion rate models used by industries are empirical as they are more adjustable with respect to operating parameters, however, mechanistic models are suggested to be more reliable because of their reliability of extrapolation to wider domains of application. In this project, we plan to use two major methods to estimate the internal corrosion rate with the actual measurements of the corrosion environments from the developed chemical sensor array, including the semi-empirical Multicorp model by using the MULTICORP software and the empirical Norsok M-506 model. In addition, ANN optimization algorithm based empirical probabilistic model may also be considered if the data is sufficient. Modification of the parameters used in these models may be needed to fully consider the effects of all the measured water/oil chemicals detected from this project.

2.2.3 Intrusive internal corrosion detection and its sensor installation methods (Questions #3 and #5)

Currently, internal corrosion detection mostly depend on the measurement of pipeline thickness changes including two general methods: intrusive and non-intrusive.[70] The intrusive method involves the installation and periodic examination of removable corrosion coupons, electrical resistance (ER) probes, and ultrasonic probes in areas of the pipeline where internal corrosion are susceptible.[71-74] To use corrosion coupons for weight loss measurements, coupon which may be a strip of metal about 75-mm long and 3.175-mm thick, made of material similar to the pipeline is weighed, then inserted into an access point, and left for at least six months. Coupons need to be placed in a holder which has to be mounted to the pipeline's interior wall or screwed at an opening fittings if applicable. Shown in Figures 19(a, b) are examples as the excalibur shield corrosion system provided by Cathodic Protection Solutions, LLC., Odessa, West Texas.[75] The installation of the corrosion coupons can follow the NACE Standard RP0775-2005 for how to prepare and insert a coupon inside the pipeline for internal corrosion detection.[76]

(a) (b)

Figure 19. Example corrosion coupon installation methods[75] (a) inserted coupon and (b) screwed coupon

In addition to the corrosion coupons, electrical resistance (ER) technique can also be used as an intrusive internal corrosion detection method. Compared with the corrosion coupon, the ER technique is more like an on-line method to detect the rate of corrosion and the extent of total metal loss.[77] Although universally applicable, the ER method is uniquely suited to corrosive environments having either poor or non-continuous electrolytes such as vapors, gases, soils, "wet" hydro-carbons, and nonaqueous liquids. An ER monitoring system consists of an instrument connected to a probe. The instrument may be permanently installed to provide continuous information,[77-79] or may be portable to gather periodic data from a number of locations. Figure 20 shows the example installation of the ER probes on pipelines for internal corrosion estimation[79] available at Metal Samples Company.

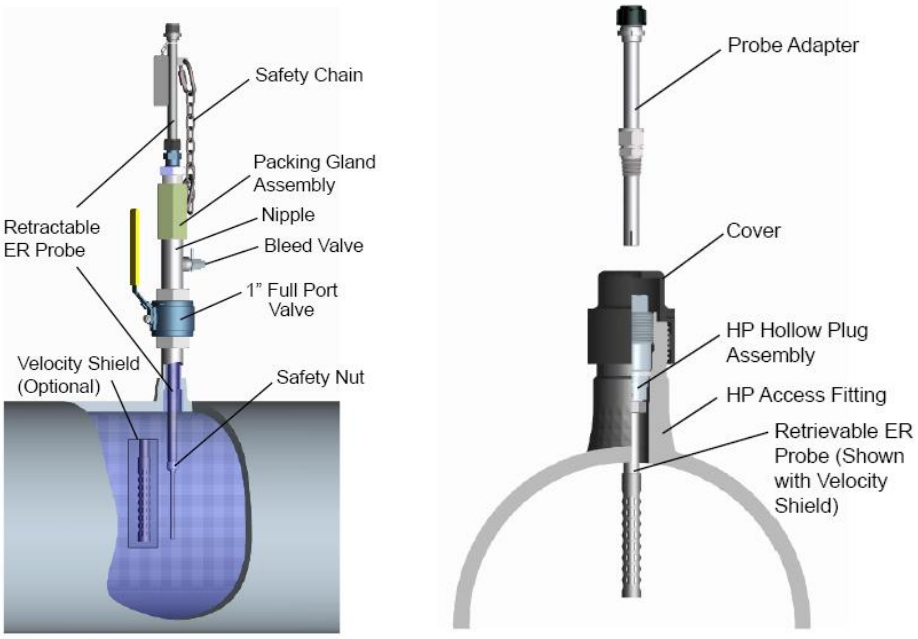

(a) (b)

Figure 20. Example electrical resistance (ER) probe installation methods (a) retractable probe and (b) retrievable probe[77]

There are some probes that can be installed externally to measure the pipeline thickness changes possibly relate to internal corrosion such as ultrasonic probes. To install an ultrasonic probe on a pipeline, the pipeline needs to be dug up then a portable device can be installed against the metal as shown in Figure 21 for an example ultrasonic probe installation from Rohrback Cosasco Systems, Inc.[78] Inside the device, voltage is applied across a piezoelectric crystal to generate an ultrasonic sound

wave that propagates through the metal. The time it takes to travel through the metal and back to the transducer is directly proportional to its thickness. Compared to the corrosion coupon and the ER probes, the ultrasonic probes do not require an injection of the probe that may introduce damages to pipelines.

Figure 21. Example ultrasonic probe installation method[78]

To overcome the limitation of the local probes, non-intrusive methods using the In-Line Inspection (ILI) tools such as Smart Pigs for piggable lines and small robots such as crawling vehicles for unpiggable lines, which can run in pipelines periodically, become an alternative option.[69,70] The applications of using the smart pigs or crawling vehicles to perform sensor installation are yet to be studied. In this project, we will try to investigate the applicability of using the visual inspection crawling vehicles to install the sensor by attaching a polymer spraying bottle on the bottom of the crawling vehicle and spraying the internal surfaces of the pipeline to install the developed chemical sensors inside the pipelines. Pipeline may need to be shut down during the installation progress.

2.2.4 Inline Inspection (ILI) Tools (Questions #1, #4, and #5)

In this project, color-change or emission-change based measurements will be performed to identify and quantify the chemical species, it is of interest to review the currently available cameras and light sources on ILI tools. In addition, the quality of images also will determine the needed dimension (size) of the sensor to be developed, which is related to the resolution of the cameras. Literature shows that visual inspection through cameras has gained growing attentions for oil/gas pipeline internal condition assessment, especially for unpiggable pipelines. There are two types of visual inspections currently available for pipeline internal condition assessment including crawling vehicles (normally has limited inspection length up to 100 m or 1000 ft. of pipeline segment per inspection) and video pigs (with no limit on inspection length). For the purpose of taking video to analyze the color/emission changes of the chemical sensor array to be developed in this project, either crawling vehicles or video pigs, as long as quality images can be recorded, can be used to record the chemical sensor color/emission changes. Operators with capability of applying field visual crawling vehicles or video pigs will be the potential candidates for future field testing of this project.

Various crawling vehicles are available for performing pipeline internal condition visual inspections. Figure 22 shows a few examples of these crawling vehicles, such as the active stereo omnidirectional vision sensor,[80] Inuktun pipeline inspection vehicle,[81] large variable geometry crawler,[82] axial symmetric light stripe sensor,[83] and the robotic crawler[84] in different sizes. As can be seen from Figure 22, most of the current visual inspection crawlers have the camera in front and with

extra cameras on the bottom of the crawlers in some cases. Since it is very dark inside the pipeline, LED light sources (two LED lights or LED light array) are commonly used (also seen in Figure 22). Figure 23 shows some example images obtained from video crawling vehicles such as remote video inspection (RVI) from Maverick,[85] axial symmetric light stripe sensor,[83] and large variable geometry crawler.[82] From these images, it can be seen that a 2″ diameter object can be easily identified from the recorded image.

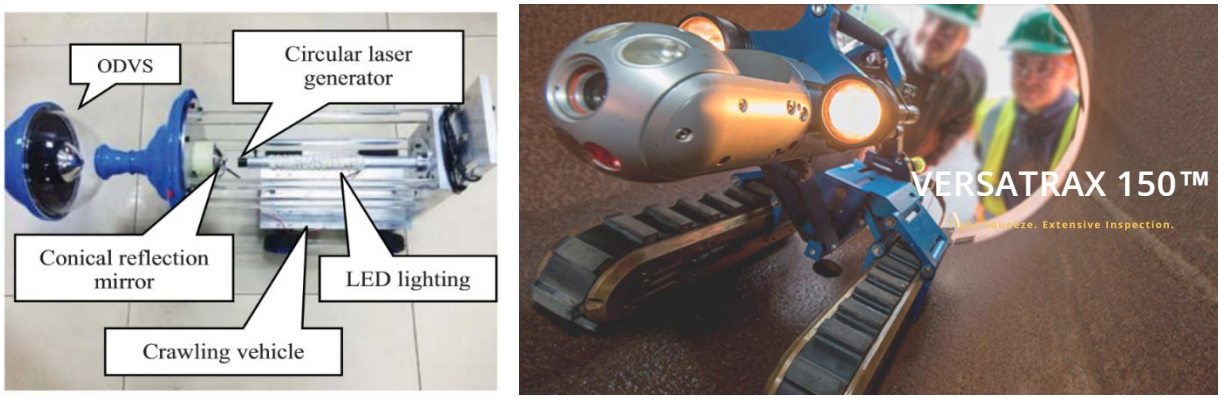

(a) (b)

(c) (d) (e)

Figure 22. ILI with cameras for pipeline inspection (a) Active Stereo Omnidirectional Vision Sensor,[80] (b) Inuktun Pipe Inspection Vehicle VERSATRAX 150,[81] (c) Large Variable Geometry Crawler (VGC),[82] (d) Axial Symmetric Light Stripe Sensor,[83] and (e) Robotic Crawler by PureRobotics[84]

(a) (b) (c)

Figure 23. Example images from (a) Remote Video Inspection (RVI),[85] (b) Axial Symmetric Light Stripe Sensor,[80] and (c) Large Variable Geometry Crawler[82]

Since most crawling vehicles need cables to run inside pipelines, it limited their application to a certain length of pipeline sections (normally within 1000 ft. or 500 m) and at a limited crawling speed (around 30 ft/s or 10 m/s). To overcome these limitations, for the piggable pipelines, some visual inspections are available using video pigs. These video pigs have internal battery and can run unlimited mileages compared to crawling vehicles. Figure 24 show example video pigs commercially available

from Dacon and Pipesurvey International.[86,87] Similar to the crawling vehicles, the camera was installed in front of the pig. Figure 25 shows some example images from the video pigs.[86] The quality of the images are similar to that obtained by the crawling vehicles. An object with 2″ in diameter can be easily detected using the recorded images from the video pigs. However, compared to the crawling vehicles, the video pigs are not as popular. Thus, limited numbers of companies offer the service.

Figure 24. Example video pigs[86]

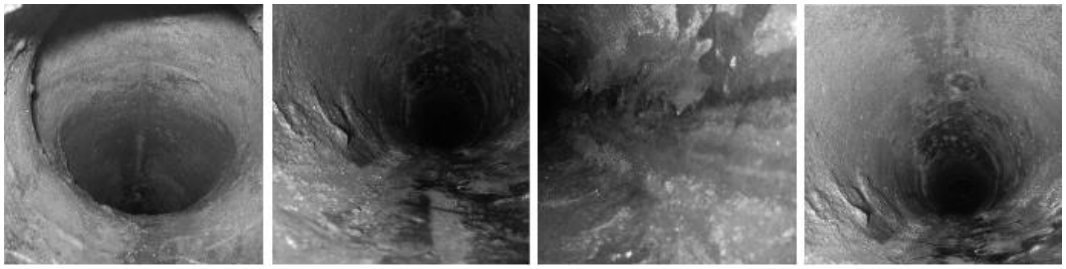

Figure 25. Example photos taken from video pigs[86]

Based on the above review, this project will use one camera in front and a LED array with four LED lights to perform image taken in laboratory to simulate the ILI crawling vehicles in field. In addition, a sensor with 2 in. × 2 in. and 4 in. × 4 in. will be initially fabricated to be installed inside the pipelines.

2.2.5 Pipeline Utility Pigs (Question #4)

In this project, the chemical sensors are expected to be installed inside the pipelines by attaching the polymer based sensors on the inner surface of the pipe. The thickness of the sensors is expected to be thin, which may be a challenge when utility pigs pass through the sensors. Because the utility pigs, including the cleaning pigs mainly used to remove accumulated solids and debris and sealing pigs utilized mostly to remove accumulated liquids, separate dissimilar fluids and dewatering, have disc sizes larger than the inner diameter of the pipe, they may cause damages to the sensors. . Cleaning pigs are[88].

According to the utility pig selection guidance, these pigs have length generally 1.5 to 2 times of the pipe's nominal diameter. All the cleaning pigs, regardless of style, are 1% to 5% oversize, and thus are larger than the pipeline internal diameter and run at a speed of 1.5-12 ft/s inside the pipeline to perform the cleaning.

The materials used for cleaning and sealing pigs depend on the application, including mainly mandrel pigs, poly pigs and foam swabs, cast urethane pigs, and spherical pigs. The bodies of mandrel pigs usually made up of either aluminum or steel. Two seals in front and rear on a mandrel pig are made of urethane, nitrile or neoprene and a mandrel pig usually has accessory brushes are shown in Figure 26 (a) as example brushes. Foam or poly pigs are versatile, flexible and usually the least expensive. They are made of open-cell polyurethane foam (see Figure 26(b) for examples). The foam may be bare (swab) or can be coated with urethane for more durability and may contain wire bristle brushes or metal studs for more abrasive cleaning. The cast urethane pigs are made of one piece urethane and offer flexibility in performance and capabilities. Spheres or ball pigs are the oldest and

most recognized sealing pigs, which are used to push liquids out of pipelines with three types of spheres including inflatable, solid, and foam.[90]

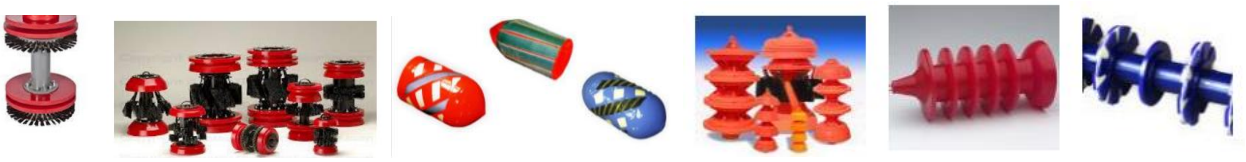

(a) (b) (c)

Figure 26. Example cleaning pigs (a) mandrel pigs, (b) foam pigs, and (c) cast urethane pigs

In this project, to validate whether the passing utility pig will damage the proposed chemical sensor array, numerical simulations using finite element analysis are needed and will be performed using various pig dimensions (1~5% oversized compared to the inner diameter of the pipe) and materials (mostly urethane and polyurethane) as mentioned above to design the best thickness and the selection of best polymer matrix to grow the chemical sensors to survive the cleaning and sealing service from the utility pigs in field applications.

2.3 Student Mentoring

During the first quarter, three graduate students (Wei Xu, Ph.D. student, Shuomang Shi, Ph. D. student, and Hafiz Usman Ahmed, masters student) and two undergraduate research assistants (Gina Blazanin and Hashem Sonbol) were hired to work on this project. All three graduate students completed their hiring process in January 2019 and will start their contract on this project in the first two weeks of January 2019. The three graduate students will work on this project from Quarter 2 to Quarter 4 of this project. The two undergraduate students were hired from October 2018 to December 2018. New undergraduate research assistants will be hired in January 2019 for the second quarter of this project.

2.4 Outreach Activities

On Oct. 24th, 2018 (8 am to 2 pm), an one-day outreach event named "Pipeline Challenge" workshop in BrainSTEM was conducted based on this project. This workshop intended to let the middle school students have hands-on experiences using easy tools to plan and build pipeline. It is expected to encourage and generate interests for young kids to pursue pipeline engineering for future college education or careers. Table 1 is the schedule of the event.

Table 1 Outreach BrainSTEM Workshop Schedule

8:00	-	9:00	Presenter Arrival
9:00	-	9:25	Student Arrival
9:25	-	9:40	Welcome in Centrum *We would like you to join us for this if possible. We'll line up the presenters in the front and do quick introductions for the kids. I'd also like a group photo*
9:50	-	10:40	Session 1
10:50	-	11:40	Session 2
11:45	-	12:25	Lunch – Anderson Commons
12:30	-	1:20	Session 3
1:20	-	1:30	Students board buses to return to Ben Franklin for keynote Sadiyo Hassan in BF auditorium

The "Pipeline Challenge" workshop contributed to all three sessions of the BrianSTEM program, with around 20 students in each session. Approximately 60 middle school students attended this workshop. Three graduate students volunteered in this outreach event to guide the middle school students. Figure 27 shows the photos taken from this event. More outreach events are planned for middle school girls in next quarter.

Figure 27. Photos from the BrianSTEM outreach event

3. Future work

In the second quarter, there will be three objectives:

1) Focus on the research activities planned in Task 2.1: Development of Colorimetric/Fluorescent Chemical Sensor Array;
2) Start numerical simulations (finite element analysis) on Task 2.2: Calibration of The Colorimetric/Fluorescent Chemical Sensor Array
3) Supervise the three graduate students in performing research Tasks 2.1 and 2.2;
4) Conduct an one-day "Pipeline Challenge" workshop outreach event in the "Expanding Your Horizons" program on March 30th, 2019 (9:00 am to 4:00 pm) to middle school girls in Grades 7, 8, and 9. Four sessions are planned in this event (around 20 students in each session, and thus approximately total 80 students).

References

1. Saleem, M.; Choi, N. G.; Lee, K. H. Facile synthesis of an optical sensor for CO_3^{2-} and HCO_3^- detection. *Intern. J. Environ. Anal. Chem.* **2015**, *95*, 592-608.
2. Lu, Y. N.; Peng, J. L.; Zhou, X.; Wu, J. Z., Ou, Y. C.; Cai, Y. P. Rapid naked-eye luminescence detection of carbonate ion through acetonitrile hydrolysis induced europium complexes. *Cryst. Eng. Comm*. **2018**, *20*, 7574-7581.
3. Hennrich, G.; Sonnenschein, H.; Resch-Genger, U. Fluorescent anion receptors with iminoylthiourea binding sites—selective hydrogen bond mediated recognition of CO_3^{2-}, HCO_3^- and HPO_4^{2-}. *Tetrahedron Letts*. **2001**, *42*, 2805-2808.
4. Han, C.; Cui, Z.; Zou, Z.; Tian, D.; Li, H. Urea-type ligand-modified CdSe quantum dots as a fluorescence "turn-on" sensor for CO_3^{2-} anions. *Photochem. Photobiol. Sci.* **2010**, *9*, 1269-1273.
5. Ghorai, A.; Mondal, J.; Chandra, R.; Patra, G. K. A reversible fluorescent-colorimetric chemosensor

based on a novel Schiff base for visual detection of CO_3^{2-} in aqueous solution. *RSC Adv*. **2016**, *6*, 72185-72192.
6. Choi, M. G.; Cha, S.; Lee, H.; Jeon, H. L.; Chang, S. K. Sulfide-selective chemosignaling by a Cu^{2+} complex of dipicolylamine appended fluorescein. *Chem. Commun*. **2009**, *47*, 7390-7392.
7. Hou, F.; Huang, L.; Xi, P.; Cheng, J.; Zhao, X.; Xie, G.; Zeng, Z. A retrievable and highly selective fluorescent probe for monitoring sulfide and imaging in living cells. *Inorg. Chem.* **2012**, *51*, 2454-2460.
8. Sasakura, K.; Hanaoka, K.; Shibuya, N.; Mikami, Y.; Kimura, Y.; Komatsu, T.; Nagano, T. Development of a highly selective fluorescence probe for hydrogen sulfide. *J. Am. Chem. Soc*. **2011**, *133*, 18003-18005.
9. Qian, Y.; Karpus, J.; Kabil, O.; Zhang, S. Y.; Zhu, H. L.; Banerjee, R.; He, C. Selective fluorescent probes for live-cell monitoring of sulphide. *Nat. Commum*. **2011**, *2*, 495.
10. Lippert, A. R.; New, E. J.; Chang, C. J. Reaction-based fluorescent probes for selective imaging of hydrogen sulfide in living cells. *J. Am. Chem. Soc*. **2011**, *133*, 10078-10080.
11. Faizi, M. S. H.; Gupta, S.; Jain, V. K.; Sen, P. Highly selective visual detection of Fe^{3+} at ppm level. *Sens. Actuators B*. **2016**, *222*, 15-20.
12. He, L.; Liu, C; Xin, J. H. A novel turn-on colorimetric and fluorescent sensor for Fe^{3+} and Al^{3+} with solvent-dependent binding properties and its sequential response to carbonate. *Sens. Actuators B.* **2015**, *213*, 181-187.
13. Xiang, Y.; Tong, A. A new rhodamine-based chemosensor exhibiting selective FeIII-amplified fluorescence. *Org. Lett*. **2006**, *8*, 1549-1552.
14. Wang, B.; Hai, J.; Liu, Z.; Wang, Q.; Yang, Z.; Sun, S. Selective Detection of Iron (III) by Rhodamine-Modified Fe_3O_4 Nanoparticles. *Angew. Chem. Int. Ed*. **2006**, *49*, 4576-4579.
15. Ji, Z.; Li, Y.; Sun, W. Acid/base sensitive platinum terpyridyl complex: Switching between metal-to-ligand charge transfer (MLCT), ligand-to-ligand charge transfer (LLCT), and intraligand charge transfer (ILCT) states. *J. Organomet. Chem.* **2009**, *694*, 4140-4145.
16. Han, M. J.; Gao, L. H.; Wang, K. Z. Ruthenium (ii) complex of 2-(9-anthryl)-1 H-imidazo [4, 5-f][1, 10] phenanthroline: synthesis, spectrophotometric pH titrations and DNA interaction. *New J. Chem*. **2006**, *30*, 208-214.
17. Bai, G. Y.; Wang, K. Z.; Duan, Z. M.; Gao, L. H. Luminescent pH sensing and DNA binding properties of a novel ruthenium (II) complex. *J. Inorg. Biochem.* **2004**, *98*, 1017-1022.
18. Chen, L.; He, L.; Ma, F.; Liu, W.; Wang, Y.; Silver, M. A.; Chai, Z. Covalent Organic Framework Functionalized with 8-Hydroxyquinoline as a Dual-Mode Fluorescent and Colorimetric pH Sensor. *ACS Appl. Mater. Interfaces*. **2018**, *10*, 15364-15368.
19. CAPP Technical Document. Recommended Practice for Mitigation of Internal Corrosion in Sour Gas Gathering System. 2003-0023, January **2003**.
20. Canadian Association of Petroleum Producers Technical Document, Recommended Practice for Mitigation of Internal Corrosion in Sweet Gas Gathering System. 2002-0013, February **2002**.
21. Papavinasam, S., Doiron, A., Revie, R. W., and Sizov, V. Special report: Corrosion modeling -1: Model predicts internal pitting corrosion of oil, gas pipelines. *Method aids execution, improves subsea equipment reliability, OGJ Newsletter*, 11/26/**2017**.
22. Papavinasam, S., Revie, R.W., Friesen, W., Doiron, A., and Panneerselvam, T. Review of Models to Predict Internal Pitting Corrosion of Oil and Gas Pipelines. *Corrosion Reviews*, **2006** 24(3-4), 173-230.
23. Nyborg, R. CO_2 corrosion model for oil and gas production systems, NACE International Corrosion Conference **2010**, Paper ID 10371.
24. Nešić, S. Key issues related to modelling of internal corrosion of oil and gas pipelines–A review. *Corrosion science*, **2007**, 49, 4308-4338.
25. De Waard, C. and Milliams, D. Carbonic acid corrosion of steel. *Corrosion*, **1975**, 31, 177-181.

26. Anderko, A. and Young, R. D. Simulation of CO_2/H_2S Corrosion Using Thermodynamic and Electro-chemical Models. *CORROSION/99*, **1999**, Paper No. 31, (Houston, TX: NACE International).
27. Anderko, A. Simulation of $FeCO_3$/FeS Scale Formation Using Thermodynamic and Electrochemical Models. In *Proceedings of the Corrosion 2000*, Orlando, FL, USA, 26–31 March 2000; NACE International: Houston, TX, USA, 2000.
28. De Waard, C., Lotz, U. and Milliams, D. Predictive model for CO_2 corrosion engineering in wet natural gas pipelines. *Corrosion*, **1991**, 47, 976-985.
29. De Waard, C., Lotz, U., and Dugstad, A. Influence of Liquid Flow Velocity on CO_2 Corrosion: A Semi -Empirical Model. *CORROSION/95*, **1995**, Paper No. 128, (Houston, TX: NACE International).
30. Dugstad, A., Lunde, L., and Videm, K. Parametric Study of CO_2 Corrosion of Carbon Steel. *CORROSION/94*, **1994**, Paper No. 14, (Houston, TX: NACE International).
31. De Waard, C., Smith, L., and Craig, B. D. The Influence of Crude Oil on Well Tubing Corrosion Rates. *CORROSION/2003*, **2003**, Paper no. 03629, (Houston, TX: NACE International, 2003).
32. Smith, L. and De Waard, C. Corrosion Prediction and Materials Selection for Oil and Gas Producing Environments. *CORROSION/2005*, **2005**, Paper no. 05648, (Houston, TX: NACE International, 2005).
33. Nordsveen, M., Nesic, S., Nyborg, R., and Stangeland, A. A Mechanistic Model for CO_2 Corrosion with Protective Iron Carbonate Films - Part 1: Theory and Verification. *Corrosion*, **2003**, 59(5), 443-456.
34. Nesic, S., Nordsveen, M., Nyborg, R., and Stangeland, A. Mechanistic Model for CO_2 Corrosion with Protective Iron Carbonate Films - Part 2: A Numerical Experiment. *Corrosion*, **2003**, 59(6), 489-497.
35. Nesic, S., Postlethwaite, J. and Olsen, S. An Electrochemical Model for Prediction of Corrosion of Mild Steel in Aqueous Carbon Dioxide Solutions. *Corrosion*, **1996**, 52(4), 280.
36. Srinivasan, S., and Kane, R. D. Prediction of Corrosivity of CO_2/ H_2S Production Environments. *CORROSION/96*, **1996**, Paper No. 11, (Houston, TX: NACE International, 1996).
37. Sangita, K. A. and Srinivasan, S. An Analytical Model to Experimentally Emulate Flow Effects in Multiphase CO_2/H_2S Systems. *CORROSION/2000*, **2000**, Paper No. 58, (Houston, TX: NACE International, 2000).
38. Srinivasan, S. and R. D. Kane, "Critical Issues in the Application and Evaluation of a Corrosion Prediction Model for Oil and Gas Systems", *CORROSION/2003*, **2003**, Paper No. 03640, (Houston, TX: NACE International, 2003).
39. Hedges, B., Chapman, R., Harrop, D., Mohammed, I., and Sun, Y. A Prophetic CO_2 Corrosion Tool - But When is it to be Believed? *CORROSION/2005*, **2005**, Paper No. 05552, (Houston, TX: NACE International, 2005).
40. Nyborg, R. Guidelines for prediction of CO_2 corrosion in oil and gas production systems. IFE/KR/E-2009/003, (Kjeller, Norway: Institute for Energy Technology, 2009).
41. Nesic, S., Wang, S., Cai, J., and Xiao, Y. Integrated CO_2 Corrosion - Multiphase Flow Model. *CORROSION/2004*, **2004**, Paper No. 04626, (Houston, TX: NACE International, 2004).
42. Nesic, S., Cai, J., and Lee, K. L. J. A Multiphase Flow and Internal Corrosion Prediction Model for Mild Steel Pipelines. *CORROSION/2005*, **2005**, Paper No. 05556, (Houston, TX: NACE International, 2005).
43. Nesic, S., Wang, S., Fang, H., Sun, W., and Lee, J. K.-L. A New Updated Model of CO_2/H_2S Corrosion in Multiphase Flow. *CORROSION/2008*, **2008**, paper no. 08535, (Houston, TX: NACE International, 2008).
44. CO_2 Corrosion Rate Calculation Model, Rev. 2., NORSOK standard No. M-506, http://www.standard.no/en/Sectors/Petroleum/NORSOK-Standard-Categories/M-Material/M-5061, (Oslo: Standards Norway, 2005).

45. ObaniJesu, E. O. Modeling the H2S Contribution to Internal Corrosion Rate of Natural Gas Pipeline, *Energy Sources, Part A: Recovery, Utilization, and Environmental Effects*, **2009**, 31(4), 348-363, DOI: 10.1080/15567030701528408.
46. Halvorsen, A. M. K. and Søntvedt, T. CO_2 Corrosion Model for Carbon Steel Including a Wall Shear Stress Model for Multiphase Flow and Limits for Production Rate to Avoid Mesa Attack. *CORROSION/99*, **1999**, Paper No. 42, (Houston, TX: NACE International, 1999).
47. Nyborg, R. and Dugstad, A. Understanding and Prediction of Mesa Corrosion Attack. *CORROSION/2003*, **2003**, Paper No. 3642, NACE International, 2003.
48. Olsen, S., Halvorsen, A. M., Lunde, P. G. , and Nyborg, R. CO_2 Corrosion Prediction Model - Basic Principles. *CORROSION/2005*, **2005**, Paper No. 05551, (Houston, TX: NACE International, 2005).
49. Gunaltun, Y., and Kopliku A. Field Data Collection, Evaluation and Use for Corrosivity Prediction and Validation of Models. Part I: Collection of Reliable Field Data for Validation of Prediction Models. *CORROSION/2006*, **2006**, Paper No. 06117, (Houston, TX: NACE International, 2006).
50. Pots, B. F. M. Mechanistic Models for the Prediction of CO_2 Corrosion Rates under Multi-Phase Flow Conditions. *CORROSION/95*, **1995**, Paper No. 137, (Houston, TX: NACE International, 1995).
51. Pots, B. F. M., John, R. C., Rippon, I. J., Thomas, M. J. J. S., Kapusta, S. D., Girgis, M. M., and Whitham, T. Improvements on de Waard - Milliams Corrosion Prediction and Applications to Corrosion Management. *CORROSION/2002*, **2002**, Paper No. 02235, (Houston, TX: NACE International, 2002).
52. Pots, B. F. M. and Kapusta, S. D. Prediction of Corrosion Rates of the Main Corrosion Mechanisms in Upstream applications. *CORROSION/2005*, **2005**, Paper No. 05550, (Houston, TX: NACE International, 2005).
53. John, R. C., Jordan, K. G., Young, A. L., Kapusta, S. D., and Thompson, W. T. SweetCor: An Information System for the Analysis of Corrosion of Steels by Water and Carbon Dioxide. *CORROSION/98*, **1998**, Paper No. 20, (Houston, TX: NACE International, 1998).
54. Nyborg, R. Field Data Collection, Evaluation and Use for Corrosivity Prediction and Validation of Models, Part II: Evaluation of Field Data and Comparison of Prediction Models. *CORROSION/2006*, **2006**, Paper no. 06118, (Houston, TX: NACE International, 2006).
55. Nyborg, R. Overview of CO_2 Corrosion Models for Wells and Pipelines. *CORROSION/2002*, **2002**, Paper No. 02233, (Houston, TX: NACE International, 2002).
56. Gunaltun, Y. M. Combining research and field data for corrosion rate prediction. *CORROSION/96*, **1996**, Paper No. 27, (Houston, TX: NACE International, 1996).
57. Wu, K. Y. and Mosleh, A. Probabilistic Model for Internal Uniform/Pitting Corrosion of Gas pipelines. Probabilistic Safety Assessment and Management PSAM 14, September 2018, Los Angeles, CA
58. Heidary, R., Gabriel, S. A., Modarres, M., Groth, K. M., and Vahdati, N. A Review of Data-Driven Oil and Gas Pipeline Pitting Corrosion Growth Models Applicable for Prognostic and Health Management. *International Journal of Prognostics and Health Management*, **2018**, ISSN 2153-2648, 2018-009
59. Shibata, T. Statistical and stochastic approaches to localized corrosion. *Corrosion*, **1996**, 52(11), 813-830. doi:10.5006/1.3292074
60. Tarantseva, K. Models and methods of forecasting pitting corrosion. *Protection of metals and physical chemistry of surfaces*, **2010**, 46(1), 139-147. doi:10.1134/S2070205110010211
61. Valor, A., Caleyo, F., Alfonso, L., Velázquez, J. C., & Hallen, J. M. Markov chain models for the stochastic modeling of pitting corrosion. *Mathematical Problems in Engineering*, **2013**, doi:10.1155/2013/108386

62. Provan, J. W., & Rodriguez III, E. S. Part I: Development of a Markov description of pitting corrosion. *Corrosion*, **1989**, 45(3), 178-192. doi:10.5006/1.3577840
63. Kexi, L., Bin, C., and Zhao, L. An Effective Internal Corrosion Rate Prediction Model for the Wet Natural Gas Gathering Pipeline. 2011 International Conference on Computational and Information Sciences, IEEE Computer Society, pp. 698-701, DOI 10.1109/ICCIS.2011.72
64. Kexi, L., Yao, Q., Wu, X., and Jia, W. A Numerical Corrosion Rate Prediction Method for Direct Assessment of Wet Gas Gathering Pipelines Internal Corrosion. *Energies* **2012**, 5, 3892-3907; doi:10.3390/en5103892
65. De Masi, G., Vichi, R., Gentile, M., and Gabetta, G. A Neural Network Predictive Model of Pipeline Internal Corrosion Profile. 2014 First International Conference on Systems Informatics, Modelling and Simulation, IEEE Computer Society, pp.18-23, DOI 10.1109/SIMS.2014.14
66. Zheng, Y., Shu, J., Ren, C., and Zhang, F. Prediction of Gathering Pipeline Internal Corrosion Rate Based on Improved Wavelet Neural Network Model, ASCE ICPTT 2011
67. Nesic, S., Nordsveen, M., Maxwell, N., and Vrhovac, M. Probabilistic modelling of CO2 corrosion laboratory data using neural networks. *Corrosion Science*, **2001**, 43 7: 1373-1392.
68. Hernández, S., Nesic, S., Weckman, G., and Ghai, V. Use of Artificial Neural Networks for Predicting Crude Oil Effect on CO_2 Corrosion of Carbon Steels. NACE Corrosion 2005 conference, Paper No. 05554, 2005
69. Gabetta, G., and Trasatti, S. P. Analysis of CO_2 corrosion model by Neural Networks. Proceedings of EUROCORR 2006, Maastricht, The Netherlands, 2006
70. Light, G. M., Kim, S. Y., Spinks, R. L., and Kwun, H. Monitoring Technology for Early Detection of Internal Corrosion for Pipeline Integirity. Final report to DOE Award Number DE-FC26-02NT41319, Sep 2003.
71. Metals Samples Company, Introduction to Corrosion Monitoring. Alabama Specialty Products, Inc., n.d. Web. 03 Dec. 2016.
72. Permasense. Comparison of Corrosion Monitoring Systems. (n.d.): n. pag. Permasense, Aug. 2015. Web. 30 Nov. 2016.
73. Metals Samples Company. Internal Corrosion Monitoring in Oil & Gas Transportation Pipeline. Alabama Specialty Products, Inc., APP NOTE - 03
74. Jarragh, A. Evaluation of the Effectiveness of Online Corrosion Monitoring Utlizing Electrical Resistance Linear Polarization Resistance Coupon within Hydrocarbon Systems. *Corrosion*, **2014**, 9-13 March, San Antonio, Texas, USA.
75. Cathodic Protection Solutions, LLC., The Excalibur Shield, https://www.cathodic-protection-solutions.com/excalibur-shield/
76. NACE Standard RP0775-2005, Recommended Practice Preparation, Installation, Analysis, and Interpretation of Corrosion Coupons in Oilfield Operations. NACE International, 2005.
77. Metal Samples Company, Electrical Resistance (ER) Monitoring, http://www.alspi.com/erintro.htm
78. Rohrback Cosasco Systems, Inc., Corrosion monitoring primer, http://www.cosasco.com/documents/Corrosion_Monitoring_Primer.pdf
79. Jarragh, A. Evaluation of the Effectiveness of Online Corrosion Monitoring Utlizing Electrical Resistance Linear Polarization Resistance Coupon Within Hydrocarbon Systems, 2014 NACE International, ISBN: 3934 2014 CP
80. Wu, T., Lu, S. and Tang, Y. An in-pipe internal defects inspection system based on the active stereo omnidirectional vision sensor. in *2015 12th International Conference on Fuzzy Systems and Knowledge Discovery, FSKD 2015*, 2016.

81. Inuktun Services Ltd., Inuktun Pipe Inspection Vehicle, Versatrax 150™, http://inuktun.com/en/products/onsite-standard-products/versatrax-150-pipe-inspection-crawler/
82. ULC Robotics., Large Variable Geometry Crawler (VGC), http://ulcrobotics.com/products/large-vgc-live-gas-main-pipeline-inspection-crawler/
83. Frey, C. W. Rotating optical geometry Sensor for fresh water pipe inspection. in *Proceedings of IEEE Sensors*, 2008, 1-4244-2581-5/08, pp. 337-340
84. Pure Technology a xylem brand, PureRobotics, https://puretechltd.com/technology/purerobotics-pipeline-inspection-system/
85. Maverick Inspection LTD., Remote Video Inspection (RVI), http://www.maverickinspection.com/services/remote-video-inspection/rvi-video-imagery-gallery/pipelines-compressors/
86. Dacon Inspection Services, Dacon Video Pigs, https://www.dacon-inspection.com/services/inspection-services/advanced-ndt/video-pigs/
87. Pipesurvey International, The In-line Video Inspection, http://www.pipesurveyinternational.com/docs/File/PIPESURVEY_Camera_Inspection.pdf, as of April 17 2018.
88. Titratsoo, J., Pipeline Pigging & Integrity Technology, 3rd Edition. Houston, TX. 2003.
89. Gibson Applied Technology and Engineering, Inc., Pipeline Pigging Part 1: Cleaning Pigs & Pigging Strategy, GAT2004-GKP-2013.01 January, 2013, pp.1-2
90. Winters, B. Cleaning pig designs and applications. NACE Central Area Conference, T. D. Williamson-Pipeline Cleaning Pigs, Houston, TX.